

# Self-induced inverse spin-Hall effect in an iron and a cobalt single-layer films themselves under the ferromagnetic resonance

Kazunari Kanagawa, Yoshio Teki, Eiji Shikoh

<b>Citation</b>	AIP Advances 8, 055910
<b>Issue Date</b>	2017-12-19
<b>Type</b>	Journal Article
<b>Textversion</b>	Publisher
<b>Rights</b>	© The Author(s). All article content, except where otherwise noted, is licensed under a Creative Commons Attribution (CC BY) license <a href="http://creativecommons.org/licenses/by/4.0/">http://creativecommons.org/licenses/by/4.0/</a> .
<b>DOI</b>	10.1063/1.5006102

Self-Archiving by Author(s)  
Placed on: Osaka City University

## Self-induced inverse spin-Hall effect in an iron and a cobalt single-layer films themselves under the ferromagnetic resonance

Kazunari Kanagawa, Yoshio Teki, and Eiji Shikoh

Citation: *AIP Advances* **8**, 055910 (2018); doi: 10.1063/1.5006102

View online: <https://doi.org/10.1063/1.5006102>

View Table of Contents: <http://aip.scitation.org/toc/adv/8/5>

Published by the [American Institute of Physics](#)

---

### Articles you may be interested in

[Conversion of spin current into charge current at room temperature: Inverse spin-Hall effect](#)  
*Applied Physics Letters* **88**, 182509 (2006); 10.1063/1.2199473

[Inverse spin-Hall effect induced by spin pumping in metallic system](#)  
*Journal of Applied Physics* **109**, 103913 (2011); 10.1063/1.3587173

[Magnetoresistance originated from charge-spin conversion in ferromagnet](#)  
*AIP Advances* **8**, 055916 (2018); 10.1063/1.5003397

[Enhanced room-temperature spin Seebeck effect in a YIG/C<sub>60</sub>/Pt layered heterostructure](#)  
*AIP Advances* **8**, 055906 (2018); 10.1063/1.5007233

[Investigation of the difference between spin Hall magnetoresistance rectification and spin pumping from the viewpoint of magnetization dynamics](#)  
*Applied Physics Letters* **112**, 092406 (2018); 10.1063/1.5017298

[Direct optical observation of spin accumulation at nonmagnetic metal/oxide interface](#)  
*Applied Physics Letters* **111**, 092402 (2017); 10.1063/1.4990113

---

**AIP** | Conference Proceedings

Get **30% off** all  
print proceedings!

Enter Promotion Code **PDF30** at checkout



## Self-induced inverse spin-Hall effect in an iron and a cobalt single-layer films themselves under the ferromagnetic resonance

Kazunari Kanagawa,<sup>1,a</sup> Yoshio Teki,<sup>2</sup> and Eiji Shikoh<sup>1,a</sup>

<sup>1</sup>Graduate School of Engineering, Osaka City University, 3-3-138 Sugimoto, Sumiyoshi-ku, Osaka 558-8585, Japan

<sup>2</sup>Graduate School of Science, Osaka City University, 3-3-138 Sugimoto, Sumiyoshi-ku, Osaka 558-8585, Japan

(Presented 9 November 2017; received 22 September 2017; accepted 31 October 2017; published online 19 December 2017)

The inverse spin-Hall effect (ISHE) is produced even in a “single-layer” ferromagnetic material film. Previously, the self-induced ISHE in a  $\text{Ni}_{80}\text{Fe}_{20}$  film under the ferromagnetic resonance (FMR) was discovered. In this study, we observed an electromotive force (EMF) in an iron (Fe) and a cobalt (Co) single-layer films themselves under the FMR. As origins of the EMFs in the films themselves, the ISHE was main for Fe and dominant for Co, respectively 2 and 18 times larger than the anomalous Hall effect. Thus, we demonstrated the self-induced ISHE in an Fe and a Co single-layer films themselves under the FMR. © 2017 Author(s). All article content, except where otherwise noted, is licensed under a Creative Commons Attribution (CC BY) license (<http://creativecommons.org/licenses/by/4.0/>). <https://doi.org/10.1063/1.5006102>

In spintronics, the spin-pumping with the ferromagnetic resonance (FMR) and the inverse spin-Hall effect (ISHE) have become powerful techniques to generate a spin current and to detect a spin current, respectively.<sup>1–13</sup> In the spin injection by using the spin-pumping with the FMR of a ferromagnetic material, the conductance mismatch problem between the ferromagnetic material and the target-material is negligible,<sup>5,6,8,9,11,13</sup> while this problem causes lowering the spin injection efficiency in cases of electrical spin injection methods.<sup>14,15</sup> The ISHE is a phenomenon that a spin current is converted to a charge current in a material due to the spin orbit interaction.<sup>1</sup> Thus, while the spin-pumping and the ISHE are fundamental, those have been applied to study the spin related properties of various materials.<sup>1–13</sup> Meanwhile, the ISHE is generated even in a ferromagnetic material “single-layer” film if a pure spin current and spin-orbit interaction exist.<sup>16</sup> Previously, in a “single-layer” ferromagnetic  $\text{Ni}_{80}\text{Fe}_{20}$  film itself formed on a thermally-oxidized silicon substrate ( $\text{SiO}_2$ -substrate), an electromotive force (EMF) due to the ISHE under the FMR was generated at room temperature.<sup>16</sup> In that case, a spin current is generated due to the two different surface ( $\text{Ni}_{80}\text{Fe}_{20}$ /air) and the bottom ( $\text{SiO}_2$ -sub./ $\text{Ni}_{80}\text{Fe}_{20}$ ) interfaces of the  $\text{Ni}_{80}\text{Fe}_{20}$  film and asymmetric spin-dependent scattering at the interfaces under the FMR condition, converted to a charge current due to the ISHE in the  $\text{Ni}_{80}\text{Fe}_{20}$  film itself, and detected as an EMF.<sup>16</sup> Until now, by using “bilayer structure” samples consisting of  $\text{Y}_3\text{Fe}_5\text{O}_{12}$  (YIG)/ $3d$ -ferromagnetic metal (FM), an EMF due to the ISHE in the  $3d$ -transition FM film has been observed with the spin-pump-induced spin injection from the YIG film into the  $3d$ -FM films.<sup>10,12</sup> However, except for the  $\text{Ni}_{80}\text{Fe}_{20}$ ,<sup>16</sup> the EMF generated in a “single-layer structure” FM film itself under the FMR has not been investigated. In this study, the EMF properties generated in an iron (Fe) single-layer and a cobalt (Co) single-layer films themselves under the FMR are investigated.

Our sample structure and experimental set up are illustrated in Figure 1. Under a vacuum pressure of  $10^{-6}$  Pa, FM (Fe, or Co) was deposited on a  $\text{SiO}_2$ -substrate to a thickness of 25 nm by using an electron-beam deposition with a deposition rate of 0.05 nm/s. After forming FM films, the sample

<sup>a</sup>Corresponding author: [kanagawa@mc.elec.eng.osaka-cu.ac.jp](mailto:kanagawa@mc.elec.eng.osaka-cu.ac.jp) (K.K.), [shikoh@elec.eng.osaka-cu.ac.jp](mailto:shikoh@elec.eng.osaka-cu.ac.jp) (E.S.)



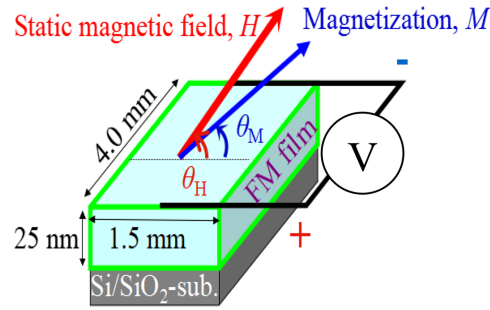


FIG. 1. A schematic illustration of our “single-layer” ferromagnetic metal (FM) film sample and experimental set up. An external static magnetic field,  $H$ , is applied with an angle,  $\theta_H$ , to the film plane.  $M$  is the magnetization vector in the FM film and  $\theta_M$  is the orientation angle of the  $M$  to the FM film plane. Two leading wires for measuring the electromotive forces from samples are attached on both ends of the FM film using silver paste.

substrates were cut as a rectangular shape of  $4.0 \times 1.5 \text{ mm}^2$  for measurements. A sample substrate was set into the microwave  $\text{TE}_{011}$ -mode cavity of an electron spin resonance (ESR) system (JEOL, JES-TE300) to excite the FMR of an FM film sample. A static magnetic field,  $H$ , was applied with an angle,  $\theta_H$ , to the sample film plane.  $M$  is the magnetization vector of the FM film and  $\theta_M$  is an orientation angle of the  $M$  to the FM film plane. The microwave frequency,  $f$ , to excite the FMR was 9.45 GHz. The EMF property of FM samples was measured by using a nano-voltmeter (Keithley Instruments, 2182A). Two leading wires to detect the output voltage properties from a sample were directly attached with silver paste at both ends of the film sample. All of the EMF measurements were done for the longitudinal direction of samples as shown in Figure 1. All of the measurements were implemented at room temperature (RT).

Figures 2(a) and (b) show FMR spectra at  $\theta_H = 0^\circ$  for an Fe sample and for a Co sample, respectively, at the microwave power to excite the respective FMR,  $P_{\text{MW}}$ , of 200 mW. FMR was

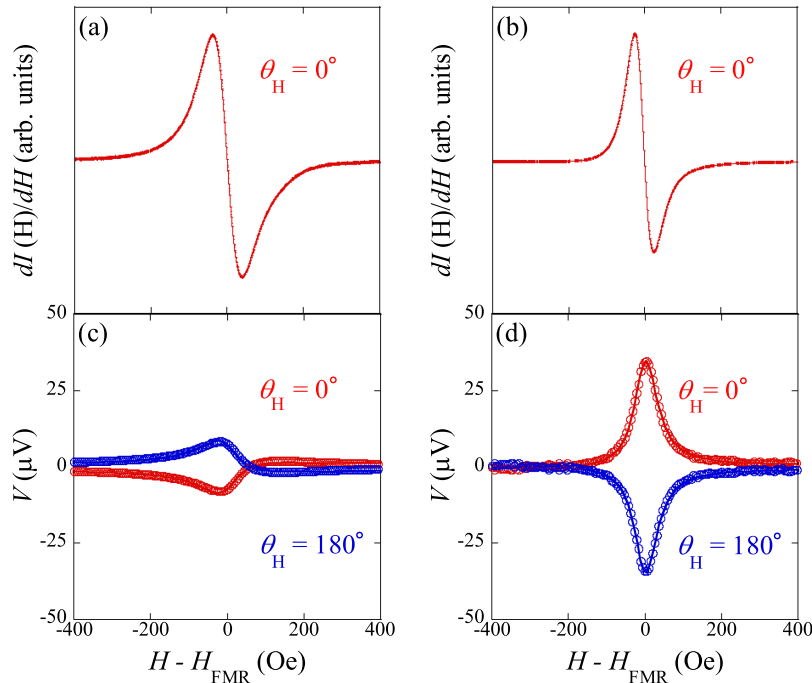


FIG. 2. FMR spectra at  $\theta_H = 0^\circ$  of (a) an Fe “single-layer” sample and (b) a Co “single-layer” sample at the microwave power of 200 mW.  $I$  is the microwave absorption intensity.  $H$  dependence of the electromotive force,  $V$ , at  $\theta_H = 0^\circ$  (red open circles and solid line) and  $180^\circ$  (blue open circles and solid line) for (c) the Fe sample and (d) the Co sample.

observed in both FM films at the respective FMR field,  $H_{\text{FMR}}$ , of 594 Oe for the Fe and 611 Oe for the Co. The saturation magnetization,  $M_S$ , was estimated to be 1330 emu/cc for the Fe and 1169 emu/cc for the Co with a general FMR condition for the case of the in-plane field:<sup>2-4</sup>

$$\omega = \gamma \sqrt{H_{\text{FMR}}(H_{\text{FMR}} + 4\pi M_S)}, \quad (1)$$

where  $\omega (= 2\pi f)$  is the angular frequency of the microwave and  $\gamma$  is the gyromagnetic ratio of the respective FMs. The estimated  $M_S$  values are comparable to other FMR experiments.<sup>17,18</sup>

Figures 2(c) and (d) show output voltage properties for the Fe sample and for the Co sample, respectively, at the  $\theta_H$  of  $0^\circ$  and  $180^\circ$  with the  $P_{\text{MW}}$  of 200 mW. The experimental data are plotted with open circles, after subtracting the components which do not depend on the  $\theta_H$  by using the following equation:

$$\overline{V(\theta_H)} = \frac{V(\theta_H) - V(\theta_H + 180^\circ)}{2}, \quad (2)$$

where the  $V(\theta_H)$  corresponds to the EMFs at the  $\theta_H$ . Using this procedure, thermal effects are ruled out except for the anomalous Nernst effect (ANE) which is discussed later. Output voltages were obtained from both FM films themselves under the respective FMR. The polarity of output voltages was inverted in both FM films against the magnetization reversal of the respective FM films. The output voltages increased with the increase of  $P_{\text{MW}}$  in both FM films. These polarity inversion of output voltages to the magnetization reversal of the FM films and the  $P_{\text{MW}}$  dependence of output voltages are almost same behaviors as previous studies using the spin-pump driven by the FMR and the ISHE.<sup>1-13,16</sup>

First, to analyze origins of those output voltage properties, the data in Figures 2(c) and (d) were fitted by the well-used following equation:<sup>1,5-9,11,13,16</sup>

$$V(H) = V_{\text{sym}} \frac{\Gamma^2}{(H - H_{\text{FMR}})^2 + \Gamma^2} + V_{\text{asym}} \frac{-2\Gamma(H - H_{\text{FMR}})}{(H - H_{\text{FMR}})^2 + \Gamma^2} + V_{\text{BG}}, \quad (3)$$

where the first and second terms of the eq. (3) correspond to the symmetry EMF to the  $H_{\text{FMR}}$  (e.g., due to the ISHE in FM films) and the anti-symmetry EMF to the  $H_{\text{FMR}}$  (e.g., due to the anomalous Hall effect (AHE) in FM films), respectively. The coefficients of  $V_{\text{sym}}$  and  $V_{\text{asym}}$  indicate the magnitudes of the symmetry and anti-symmetry EMFs to the  $H_{\text{FMR}}$ , respectively.  $\Gamma$  is a damping constant in these fittings.  $V_{\text{BG}}$  is background signals on experiments which are independent of the  $H$ . The fitting results are drawn with solid lines in Figs. 2(c) and (d). The absolute value of the  $V_{\text{sym}}$  to  $V_{\text{asym}}$  ratio,  $|V_{\text{sym}} / V_{\text{asym}}|$ , are 2 for the Fe sample and 18 for the Co sample. That is, the symmetry term is main as contribution of the generated EMFs in an Fe single-layer and dominant as contribution of the generated EMFs in a Co single-layer. The polarity of the output voltages are positive in Co and negative in Fe. This polarity difference will be described later.

Polarity inversion of  $V_{\text{sym}}$  and  $V_{\text{asym}}$  are due to the magnetization reversal of the FM films and the  $V_{\text{sym}}$  and  $V_{\text{asym}}$  depend on  $P_{\text{MW}}$ . From previous studies,<sup>4,7,9,11,16</sup> we decide that the origin of the  $V_{\text{asym}}$  is the AHE. However, at this stage, it has not been yet confirmed that the main origin of the  $V_{\text{sym}}$  is the ISHE because the planer Hall effect (PHE) and the ANE may be affected.<sup>16,19</sup> To confirm that the main origin of the  $V_{\text{sym}}$  is the self-induced ISHE indicated in the FM, first, the EMF properties were analyzed taking the PHE into account.<sup>16,19</sup> The EMF due to the PHE,  $V_{\text{PHE}}$ , is parasitically affected in our experimental configuration and estimated with the following equation:<sup>3,16</sup>

$$V_{\text{PHE}} = -\frac{1}{2} w J_1 \rho_A \cos \theta_M \frac{h\gamma \left\{ 2\alpha\omega \cos \varphi - \left[ 4\pi M_S \gamma \cos^2 \theta_M + \sqrt{(4\pi M_S)^2 \gamma^2 \cos^4 \theta_M + 4\omega^2} \right] \sin \varphi \right\}}{2\alpha\omega \sqrt{(4\pi M_S)^2 \gamma^2 \cos^4 \theta_M + 4\omega^2}}, \quad (4)$$

where  $w$ ,  $J_1$ ,  $\rho_A$ ,  $h$ ,  $\alpha$ , and  $\varphi$  are the sample width (1.5 mm), the inductive charge current, the anisotropic resistivity, the amplitude of the rf magnetic field, the Gilbert damping constant of the FM film which is proportional to the FMR spectral width, and the phase angle between the rf magnetization

and the rf current, respectively.  $\theta_M$  is estimated using the following relationship with  $\theta_H$ ,  $H_{\text{FMR}}$ , and  $M_S$ :<sup>3,16</sup>

$$H_{\text{FMR}} \sin(\theta_H - \theta_M) = 4\pi M_S \sin \theta_M \cos \theta_M. \quad (5)$$

Figures 3 (a) and (b) show the  $\theta_H$  dependence of the  $V_{\text{PHE}}$  values for an Fe sample and for a Co sample calculated by the eq. (4). Here, from the equation of electromagnetic induction and the definition of  $\varphi$ ,  $J_1$  and  $\varphi$  were examined from  $1.0 \times 10^8$  A/m<sup>2</sup> to  $1.0 \times 10^{10}$  A/m<sup>2</sup> and from  $0^\circ$  to  $1.0^\circ$ , respectively. As a result,  $J_1$  and  $\varphi$  for the Fe were set to be  $4.0 \times 10^8$  A/m<sup>2</sup> and  $0.155^\circ$ , respectively. For the Co,  $J_1$  and  $\varphi$  were set  $1.0 \times 10^9$  A/m<sup>2</sup> and  $0.155^\circ$ , respectively.  $h$  is 0.016 Oe at the  $P_{\text{MW}}$  of 200 mW.  $\rho_A$  was experimentally estimated to be 72.0  $\mu\Omega\text{cm}$  for the Fe and 42.0  $\mu\Omega\text{cm}$  for the Co.

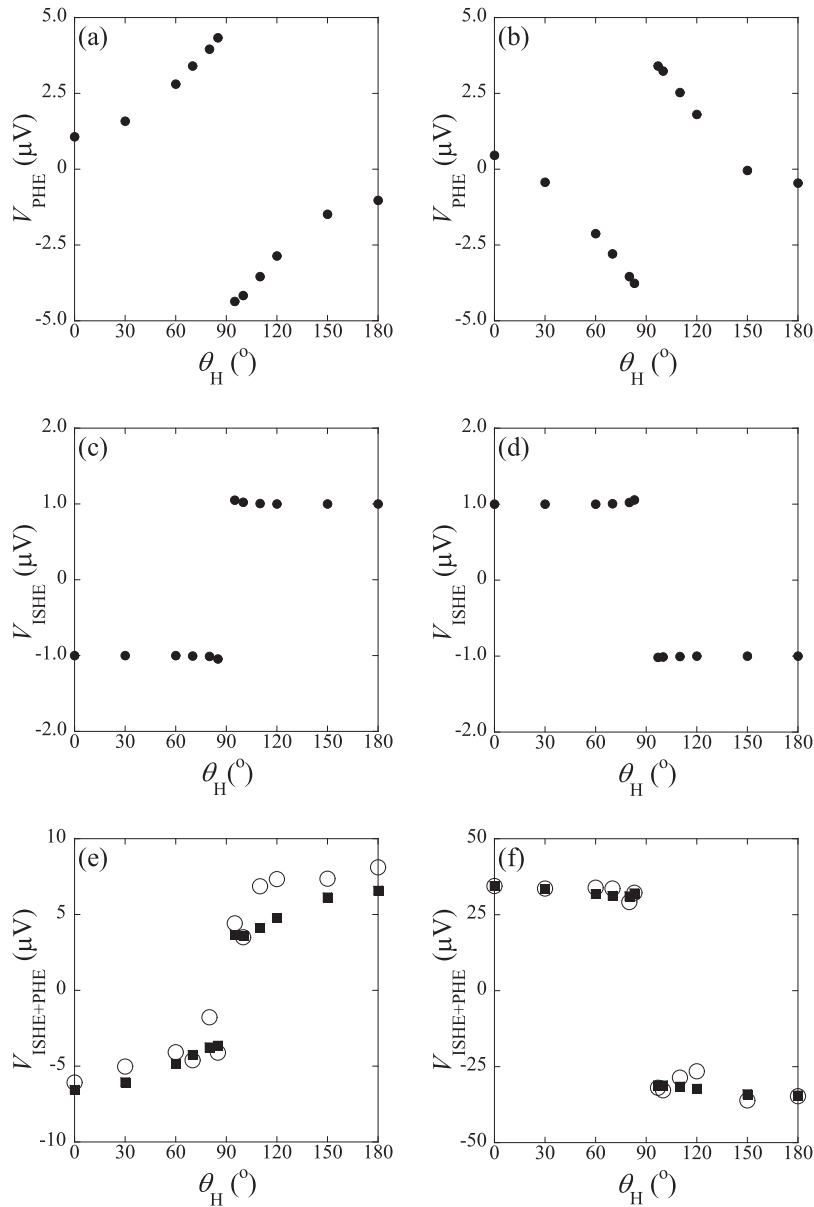


FIG. 3.  $\theta_H$  dependence of the calculated planer Hall effect (PHE) for (a) an Fe sample and (b) a Co sample.  $\theta_H$  dependence of the normalized inverse spin-Hall effect (ISHE) calculated for (c) an Fe sample and (d) a Co sample. Comparison between the experimentally obtained  $V_{\text{sym}}$  (open circles) and the calculated obtained  $V_{\text{sym}}$  (solid squares) for (e) an Fe sample and (f) a Co sample.

The  $\theta_H$  dependence of the EMF due to the ISHE,  $V_{ISHE}$ , is described as follows:<sup>3,16</sup>

$$\begin{aligned} V_{ISHE}(\theta_H) &= V_{ISHE}(\theta_H = 0^\circ) \times \overline{J_S} \\ &= V_{ISHE}(\theta_H = 0^\circ) \times \frac{2\omega \left[ 4\pi M_S \gamma \cos^2 \theta_M + \sqrt{(4\pi M_S)^2 \gamma^2 \cos^4 \theta_M + 4\omega^2} \right]}{(4\pi M_S)^2 \gamma^2 \cos^4 \theta_M + 4\omega^2}, \end{aligned} \quad (6)$$

where  $\overline{J_S} = J_S(\theta_M)/J_S(\theta_M = 0^\circ)$  is the normalized spin current density, and the calculation results of  $V_{ISHE}$  for the Fe and for the Co are shown in Figs. 3(c) and (d), respectively.

Experimentally obtained  $V_{sym}$  (circles) and calculated data (squares) for the Fe sample are plotted in Fig. 3(e), where the  $V_{ISHE} : V_{PHE}$  for the calculated data is set to be 7 : 1. Fig. 3(e) indicates the self-induced ISHE is large enough to distinguish with the PHE in Fe single-layer film. For the Co sample, similarly, the experimentally obtained  $V_{sym}$  (circles) and the calculated data (squares) are plotted in Fig. 3(f), where the  $V_{ISHE} : V_{PHE}$  is set to be 73 : 1. Fig. 3(f) indicates the self-induced  $V_{ISHE}$  is large enough to distinguish with the PHE in Co single layer film, too. Thus, the PHE is not main origin of the  $V_{sym}$  in both cases of Fe and Co films. For the second analysis, we mention the possibility that the ANE is dominant origin of the observed  $V_{sym}$ . The ANE is due to a microwave-induced temperature gradient in samples under the FMR. Under the FMR, a microwave induces thermal agitation in a sample and the sample temperature in the microwave cavity increases. The temperature gradient, vertical to the film plane, generates a charge current flow in the FM, yielding a lateral EMF, perpendicular to the magnetization of the FM film due to the ANE. Significantly, the  $\theta_H$  dependence of the EMF due to the ANE exhibits the same behavior as the  $V_{sym}$  observed in this study. Here, we note that the thermal conductivity for SiO<sub>2</sub> (substrates) and air (adjacent to the surface of the FM films) are 1.2 and 0.026 W/mK.<sup>20,21</sup> Meanwhile, for a control experiment, we prepared the samples with a Au cap layer (1~10 nm in thick) on the surface of the FM, where the thermal conductivity of a Au film is 178 W/mK.<sup>20</sup> Thus, if the ANE is dominant effect for the lateral  $V_{sym}$ , the polarity of the  $V_{sym}$  is inverted between the samples with and without a Au cap layer. However, the polarity of the EMF were not changed between the samples with and without a Au cap layer. To make sure, we estimated the influence of the ISHE in Au with the spin-Hall angle and the linewidth in the FMR spectra. As the estimation results, the amount of the ISHE in Au was under the measurement limit. Thus, the above things suggest that the ANE can also be ruled out. Thus, we demonstrated self-induced ISHE in an Fe and a Co “single-layer” films themselves under the FMR. These results are for typical FM materials and pave a way for high frequency spintronics.

Finally, we mention about the polarity of the  $V_{ISHE}$ . Under an assumption of the same experimental configuration, the polarities of the observed  $V_{ISHE}$  of 3d-FM films are different among the experimental research groups.<sup>10,12</sup> The  $V_{ISHE}$  is proportional to the magnitude of the spin current and the spin-Hall angle,  $\theta_{SH}$ . Here,  $\theta_{SH}$  is a conversion efficiency from a spin current to a charge current in the regime of the ISHE. In a theory by using a tight-binding model with a rigid band, both  $\theta_{SH}$ s of Fe and Co are positive.<sup>22</sup> In our study, the generated  $V_{ISHE}$  of the Fe sample is negative, while that of the Co sample is positive. We have confirmed the reproducibility of these experimental results. Thus, if the both  $\theta_{SH}$  of Fe and Co are positive in our study, the direction of the spin current flow may be opposite to each other. This phenomenon will be clarified by experiments to confirm the direction of spin current flow.

In summary, we have investigated EMF properties observed in an Fe and a Co “single-layer” films under the FMR. We succeeded in clarifying the origin of EMF on Fe or Co single layer. The self-induced ISHE was main origin of the observed EMFs in Fe and dominant origin of the observed EMFs in Co.

This research was partly supported by a Grant-in-Aid from the Japan Society for the Promotion of Science (JSPS) for Scientific Research (B) (26286039).

<sup>1</sup> E. Saitoh, M. Ueda, H. Miyajima, and G. Tatara, *Appl. Phys. Lett.* **88**, 182509 (2006).

<sup>2</sup> K. Ando, Y. Kajiwara, S. Takahashi, S. Maekawa, K. Takemoto, M. Takatsu, and E. Saitoh, *Phys. Rev. B* **78**, 014413 (2008).

<sup>3</sup> K. Ando and E. Saitoh, *J. Appl. Phys.* **108**, 113925 (2010).

<sup>4</sup> K. Ando, S. Takahashi, J. Ieda, Y. Kajiwara, H. Nakayama, T. Yoshino, K. Harii, Y. Fujikawa, M. Matsuo, S. Maekawa, and E. Saitoh, *J. Appl. Phys.* **109**, 103913 (2011).

- <sup>5</sup> K. Ando and E. Saitoh, *Nat. Commun.* **3**, 629 (2012).
- <sup>6</sup> E. Shikoh, K. Ando, K. Kubo, E. Saitoh, T. Shinjo, and M. Shiraishi, *Phys. Rev. Lett.* **110**, 127201 (2013).
- <sup>7</sup> Y. Kitamura, E. Shikoh, Y. Ando, T. Shinjo, and M. Shiraishi, *Sci. Rep.* **3**, 1739 (2013).
- <sup>8</sup> Z. Tang, E. Shikoh, H. Ago, K. Kawahara, Y. Ando, T. Shinjo, and M. Shiraishi, *Phys. Rev. B* **87**, 140101(R) (2013).
- <sup>9</sup> J. C. Rojas-Sánchez, M. Cubukcu, A. Jain, C. Vergnaud, C. Portemont, C. Ducruet, A. Marty, L. Vila, J.-P. Attané, E. Augendre, G. Desfonds, S. Gambarelli, G. Jaffrès, J.-M. George, and M. Jamet, *Phys. Rev. B* **88**, 064403 (2013).
- <sup>10</sup> B. F. Miao, S. Y. Huang, D. Qu, and C. L. Chien, *Phys. Rev. Lett.* **111**, 066602 (2013).
- <sup>11</sup> Y. Ando, K. Ichiba, S. Yamada, E. Shikoh, T. Shinjo, K. Hamaya, and M. Shiraishi, *Phys. Rev. B* **88**, 140406(R) (2013).
- <sup>12</sup> H. Wang, C. Du, P. C. Hammel, and F. Yang, *Appl. Phys. Lett.* **104**, 202405 (2014).
- <sup>13</sup> Y. Tani, Y. Teki, and E. Shikoh, *Appl. Phys. Lett.* **107**, 242406 (2015).
- <sup>14</sup> G. Schmidt, D. Ferrand, L. W. Molenkamp, A. T. Filip, and B. J. van Wees, *Phys. Rev. B* **62**, R4790 (2000).
- <sup>15</sup> A. Fert and H. Jaffrès, *Phys. Rev. B* **64**, 184420 (2001).
- <sup>16</sup> A. Tsukahara, Y. Ando, Y. Kitamura, H. Emoto, E. Shikoh, M. P. Delmo, T. Shinjo, and M. Shiraishi, *Phys. Rev. B* **89**, 235317 (2014).
- <sup>17</sup> E. Shikoh, Y. Ando, and T. Miyazaki, *J. Appl. Phys.* **97**, 10D501 (2005).
- <sup>18</sup> J.-M. L. Beaujour, W. Chen, A. D. Kent, and J. Z. Sun, *J. Appl. Phys.* **99**, 08N503 (2006).
- <sup>19</sup> L. Chen, S. Ikeda, F. Matsukura, and H. Ohno, *Appl. Phys. Exp.* **7**, 013002 (2014).
- <sup>20</sup> R. Kato and I. Hatta, *Int. J. Thermophys* **26**, 179 (2005).
- <sup>21</sup> E. W. Lemmon and R. T. Jacobsen, *Int. J. Thermophys* **25**, 21 (2004).
- <sup>22</sup> T. Naito, D. S. Hirashima, and H. Kontani, *Phys. Rev. B* **81**, 195111 (2010).